Supporting Information

Experimental and FEM simulation study of compressive deformation of solder microballs and particle chains

Y. Harkavyi[1], K. Giżyński[2] and Z. Rozynek,[1,3*]

[1] *Faculty of Physics, Adam Mickiewicz University, Uniwersytetu Poznańskiego 2, 61-614 Poznań, Poland*
[2] *Institute of Physical Chemistry, Polish Academy of Sciences, Kasprzaka 44/52, 01-224 Warsaw, Poland*
[3] *CADENAS P.S.A., Prof. Sylwestra Kaliskiego 24, 85-796 Bydgoszcz, Poland*

*Corresponding author: zbiroz@amu.edu.pl

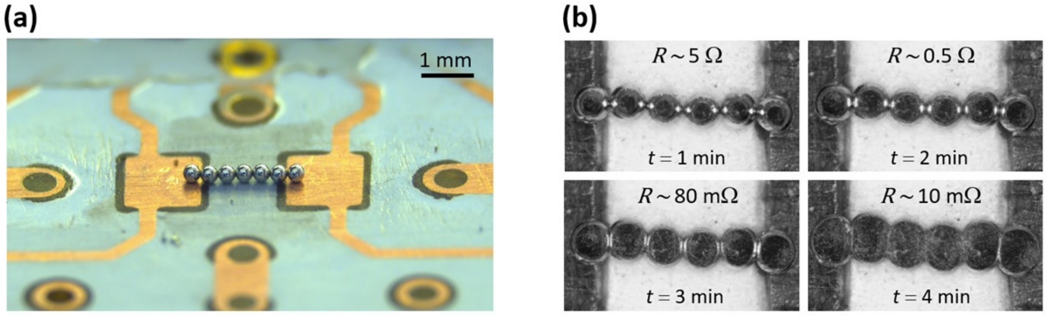

Figure S1. (**a**) Image showing a particle chain of 300-µm $Sn_{63}Pb_{37}$ spheres on a PCB carrier, stretched between two copper pads. (b) Top-view images of the compressed chain at four different stages, corresponding to 3%, 6%, 22%, and 50% compressive strain, during which the resistance of the structure changes from 5 Ω to 10 mΩ.

Resistance measurements were conducted with a Zurich Instruments MFIA (5 MHz Impedance Analyzer) using an MFITF fixture and a specially designed, low-loss PCB carrier, minimizing parasitic effects by eliminating lead wires for precise particle chain measurements. Nearly monodisperse 300-µm particles were deposited between 1.5 × 1.5 mm copper pads, 1.4 mm apart on the PCB. Low-frequency (100 Hz, 0.3 V) measurements of the impedance's real part (R) were used to minimize dielectric loss effects.

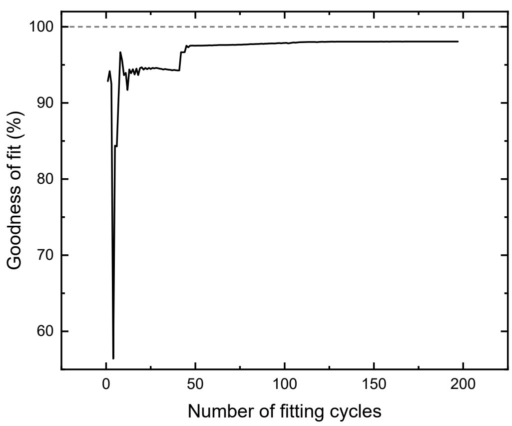

Figure S2. Goodness of fit as a function of fitting cycles during parameter optimization for the Johnson-Cook model. The goodness of fit increases sharply in the initial cycles and then gradually approaches an asymptote near 100%, where further improvements become marginal. The dashed line at 100% represents an ideal fit. This trend highlights the progressive fine-tuning of model parameters to closely align with experimental data, achieving an optimal fit within approximately 100 cycles, after which the changes stabilize.

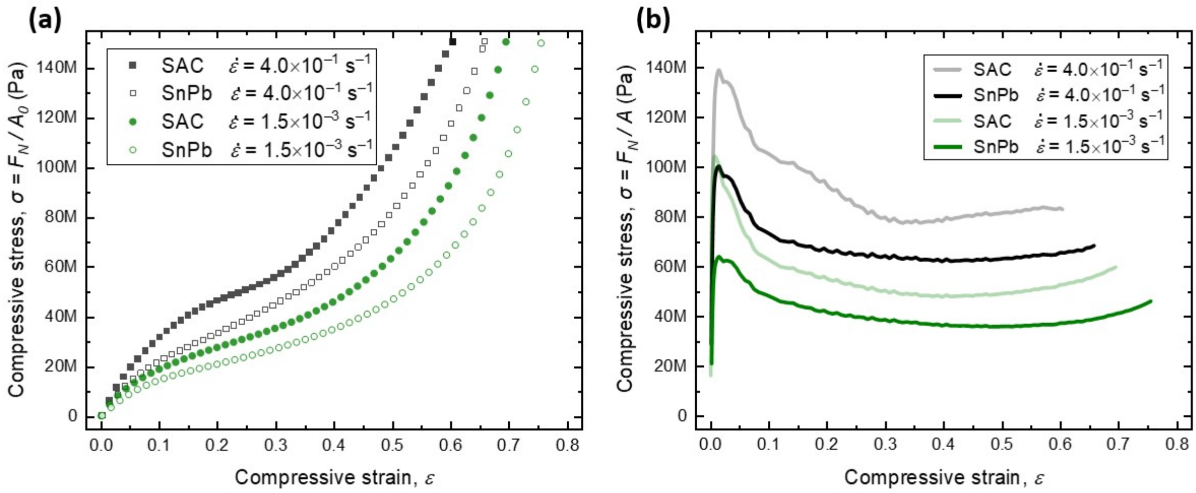

Figure S3. Compressive stress-strain curves for leaded and unleaded solder balls (**a**) Stress is calculated as applied force divided by the initial (equatorial) cross-sectional area of the uncompressed sphere. (**b**) Stress is presented as force divided by the actual contact area between the compressive slab and the sphere, which corresponds to a classical pressure-based approach.

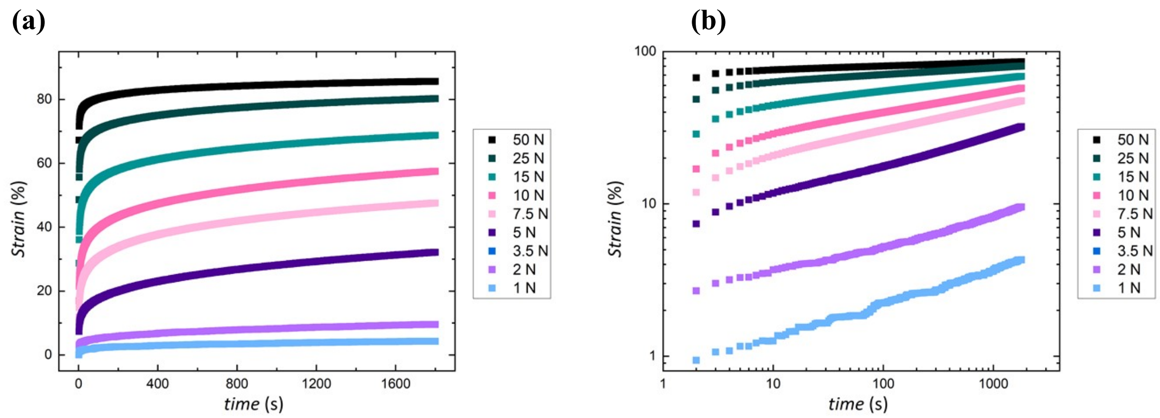

Figure S4. Engineering strain of a $Sn_{63}Pb_{37}$ solder ball with a diameter of 600 μm as a function of time, presented on (**a**) a linear-linear scale and (**b**) a log-log scale, under different compression forces (F_N) at a temperature of 23°C. The initial strain increases rapidly and then stabilizes over time, indicating a gradual approach to equilibrium. This behavior is typical for viscoelastic materials, where the material initially resists deformation and then enters a flow state.

Movie S1. 2D simulation results illustrating equivalent (local) stress distributions within a quarter-sphere subjected to uniaxial compression. The left panel shows results for a perfectly plastic material model, while the right panel presents results for a Ludwik material model.

Movie S2. 2D simulation results displaying the distribution of equivalent (local) stress (left panel) and local strain rate (right panel) within a symmetrical section of a sphere under uniaxial compression. The simulation employs the J-C model with an applied engineering strain rate of 0.1 s^{-1}.

Movie S3. 3D simulation results illustrating the stages of shape deformation for $Sn_{63}Pb_{37}$ particles under compression in two different configurations: two particles in contact (left panel) and a segment of an infinitely long particle chain (right panel). Contact areas between neighboring particles are highlighted in blue (A_2).